JMEPEG (2012) 21:137–142
DOI: 10.1007/s11665-010-9788-9

1059-9495/$19.00

Study of Residual Stress and Surface Morphology Changes in Al_2O_3 Induced by Nd:YAG Laser Irradiation

Sunmog Yeo, Sung-Ki Hong, Sung-Jun Lee, Changhwan Lim, and Jae-Won Park

(Submitted May 19, 2010; in revised form September 15, 2010)

In this study, the residual stress and surface morphology changes in alumina plates by the irradiation of a Q-switched Nd:YAG laser were investigated. The results of x-ray diffraction using the $\sin^2\psi$ technique show that laser irradiation induces tensile residual stresses on the surface of the plates, which increase with the increasing energy density of the laser beam. Residual stress and surface morphology are sensitive to the irradiation conditions. The surface morphology of the plates systematically changed with the laser energy density and the presence of an aluminum foil or water on the plates. The physical reasons for these changes are discussed in this article.

Keywords alumina, Nd:YAG laser, residual stress, surface morphology

1. Introduction

Alumina (Al_2O_3) is one of the typical refractory ceramics having high thermal shock strength and a high resistance to corrosion and erosion. Therefore, Al_2O_3 is utilized in various applications such as space planes, fusion reactors, gas turbines, and incinerators. Moreover, the laser surface treatment of Al_2O_3 can yield a pore-free, homogenous, and crack-free surface, which has a low permeability to corrosive species and a high surface hardness, and hence an increased corrosion and erosion resistance (Ref 1). The main factors affecting corrosion and erosion resistance are composition, oxygen content, and surface morphology (Ref 2, 3). Though laser irradiation cannot change the composition and oxygen content significantly, it can affect the surface morphology or surface roughness by sealing pores and eliminating surface flaws and crack homogenization macroscopically (Ref 4-6). Since the decrease in the surface roughness due to the densification and elimination of surface defects causes an increase in corrosion and erosion resistance, a study of the surface morphology provides information on important properties of ceramics. However, very few surface morphology studies have been carried out at the grain size level using a Q-switched Nd:YAG laser under various irradiation conditions.

Residual stress is also an important property of ceramics. It is related to various mechanical properties such as crack propagation, fatigue strength, and corrosion cracking. Furthermore, residual stress is one of the essential factors determining the thin film quality. For example, residual compressive stress causes the delamination of the surface layer from the substrate, while residual tensile stress may cause the formation of a surface crack in films (Ref 7, 8). Many techniques are used to investigate residual stress, such as x-ray diffraction (Ref 9, 10), nanoindentation fracture (Ref 11), Raman spectroscopy (Ref 12, 13), confocal photostimulated microspectroscopy (Ref 14), and object-oriented finite element analysis (Ref 15). Among these, x-ray diffraction is a nondestructive method and one of the most frequently used methods. In this study, a systematic investigation of residual stress changes is carried out using an x-ray diffraction method by controlling the wavelength and energy density of a Q-switched Nd:YAG laser. Furthermore, the effects of various irradiation conditions on Al_2O_3 grains in a few microsize levels are investigated through scanning electron microscope (SEM) images.

Sunmog Yeo, Sung-Ki Hong, Changhwan Lim, and **Jae-Won Park**, KAERI, PEFP, Daejeon, South Korea; and **Sung-Jun Lee**, Division of Physical Metrology, Korea Research Institute of Standards and Science, Daejeon, South Korea. Contact e-mail: sunmog@gmail.com.

2. Experiment

2.1 Measurement of X-ray Diffraction and Surface Morphology

A Rigaku x-ray diffractometer with Cu Kα radiation was used to evaluate the residual stress before and after the laser irradiation of the samples. High-purity alumina (Al_2O_3) plates (Sumitomo Chemical Co., Ltd., Osaka, Japan) with dimensions of $20 \times 50 \times 1$ mm were used as the samples. These plates were manufactured using a grinding machine. An x-ray radiation source of Cu $K\alpha_1$ (wavelength: 1.5406 Å) was used at 40 kV and 20 mA. The (1310) peak around 127.7° was selected for the residual stress analysis because the higher 2θ peaks are more sensitive to strains (or stress). θ-2θ scans were performed in the step mode wherein the data acquisition time was 30 s at every data point. Surface morphology images were obtained using the SEM (JSM 5200, JEOL) in a high vacuum state. Since Al_2O_3 is an insulator, all the alumina plates used for SEM experiments had to be coated with metallic materials to eliminate the charging effect. In the experiments described here, the plates were coated with gold using sputtering equipment (Fine Coat Ion Sputter JFC-1000) in a vacuum. The surface roughness of the samples was measured by white-light scanning interferometry (NV-3000, NanoSystem).

2.2 Laser Irradiation

Figure 1 shows the experimental setup for the residual stress control of Al_2O_3 by laser irradiation. A Q-switched Nd:YAG laser (Quanta-Ray Pro-230, $\lambda = 1064$ nm) was used as a source. By means of a second harmonic generator (SHG) with a nonlinear optical crystal, a frequency-doubled fundamental wave of a Q-switched Nd:YAG laser can be generated; this is a water-penetrable wave ($\lambda = 532$ nm). A serrated aperture was placed in front of a vacuum spatial filter to improve the beam spatial profile and image relay. The beam transmitted through the serrated aperture was propagated through a 1.4 times magnifying vacuum spatial filter. The laser beam was focused by a lens and irradiated on a test sample in a water jacket (or no water jacket for $\lambda = 1064$ nm) through a window. The test sample was fixed on a sample holder and moved along the *x*- and *y*-directions in the water jacket during laser irradiation. For $\lambda = 1064$ nm experiments, the alumina plates were enveloped by aluminum (Al) foils, instead of a water jacket, to reduce surface damage. The thermal conductivity of Al foils is 235 W/mK. Laser pulses with a pulse energy of 10-100 mJ were incident on the sample surface with a focal spot waist of 1 mm, a pulse duration of 10 ns, and a repetition rate of 10 Hz. The spot size was measured by a beam profiler (Newport LBP-1-USB). The sample holder speeds along the *x*- and *y*-directions were 1 and 0.2 mm/s, respectively. To control the experimental conditions, the laser pulse energy and beam profile (including the spot size) were monitored using an energy meter (Coherent J25LP) and a beam profiler (Newport LBP-1-USB), respectively.

2.3 Residual Stress Analysis

Since selecting the appropriate angle is important for the residual stress analysis, the x-ray diffraction experiments on the Al_2O_3 plates are performed up to $2\theta = 135°$, as shown in Fig. 2(a). All the peaks in the diffraction patterns are well defined by the Al_2O_3 polycrystalline peaks, indicating that the alumina plates do not include any significant impurity that affects the residual stress analysis. For a more precise residual stress analysis, the (1310) peak around 127.7° is chosen because this peak is well separated from the other Al_2O_3 polycrystalline peaks. In addition, this peak is located at a high angle and, hence, the Cu $K\alpha_2$ peak is well separated from the Cu $K\alpha_1$ peak. Furthermore, when a peak is located at high

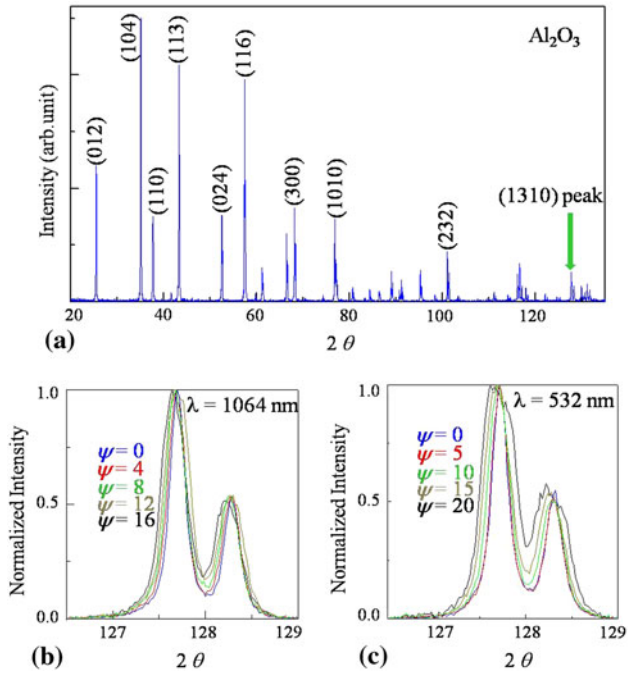

Fig. 2 X-ray diffraction pattern for residual stress analysis. (a) θ-2θ scan for alumina plates. An example of the x-ray diffraction pattern for residual stress using the wavelengths (b) 1064 nm and (c) 532 nm

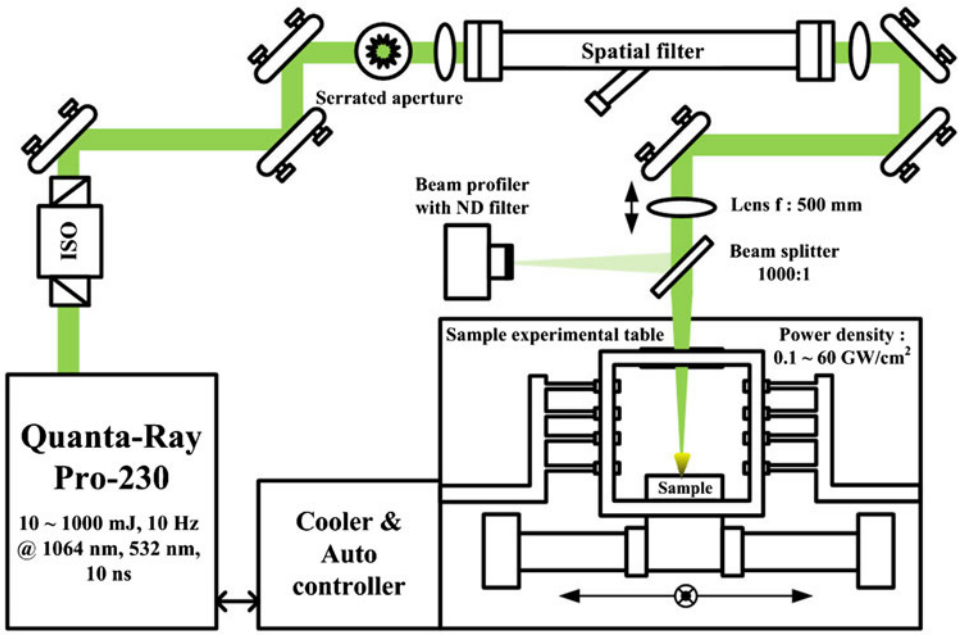

Fig. 1 Experimental set-up for residual stress control of Al_2O_3 by laser irradiation

angles, the sample angle (θ) can be tilted to higher angles for residual stress measurements, suggesting more reliable residual stress analysis due to the availability of more data points. In this article, ψ denotes the tilting angle of the sample. For the residual stress analysis, the x-ray background is removed by linear fitting and the Cu $K\alpha_1$ peaks are normalized. Figure 2(b) and (c) shows examples of residual stress measurement using x-ray diffraction patterns for the wavelengths λ = 1064 and 532 nm, respectively.

The residual stresses (σ_ϕ) are evaluated by the $\sin^2\psi$ technique (Ref 9), which is one of the most widely used techniques. It is essential to obtain precise peak positions for the $\sin^2\psi$ technique. In order to remove the Cu $K\alpha_2$ peak contributions, the Rachinger correction (Ref 16) should be applied. However, since the Cu $K\alpha_2$ peak is well separated from the Cu $K\alpha_1$ peak, there is no significant difference between the peak positions obtained with and without the Rachinger correction. Peak positions are determined for all ψ data by parabola fitting using the top 15% rule, which is an empirical rule that states the x-ray data points corresponding to 85% of the maximum intensity should be fitted by a parabola function (Ref 17). From these peak positions (2θ), the interplanar spacing (d_ψ) for every ψ can be obtained using the Bragg condition as follows: $d_\psi = \frac{1.5406}{2\sin\theta}$ (Å). The residual stress σ_ϕ can be obtained from the slope (a) of d_ψ plotted as a function of $\sin^2\psi$. Residual stress can be expressed as

$$\sigma_\phi = \frac{E}{d_0(1+\nu)} \cdot a \qquad \text{(Eq 1)}$$

where E and ν are elastic modulus and Poisson's ratio, respectively. The elastic modulus and Poisson's ratio of Al_2O_3 are ~300 and ~0.33 GPa, respectively (Ref 18). In practice, the unstressed lattice spacing (d_0) is replaced by the lattice spacing measured at ψ = 0 (Ref 9).

3. Results and Discussions

3.1 Residual Stress

Figure 3 shows a plot of interplanar spacing as a function of $\sin^2\psi$ for the alumina plates irradiated with different energy densities. According to Eq 1, the residual stresses of the alumina plates are determined by the slopes of $d_\psi(\sin^2\psi)$, which systematically increase with the increasing energy density (ε) of the laser. It is important to note that a positive slope of $d_\psi(\sin^2\psi)$ corresponds to tensile residual stress, whereas a negative slope corresponds to a compressive residual stress. The as-received alumina plate also has tensile residual stress (~257 MPa) due to the grinding process in the manufacturing stage (Ref 19). The inset of Fig. 3 summarizes the relation between the energy density and the stresses of the plates; the higher the energy density, the higher is the tensile stress induced. A compressive stress on a surface can be achieved by infiltrating some materials on the surface. In contrast, a tensile stress on a surface can be achieved by removing some materials on the surface. Basically, a laser irradiation transfers thermal energy on the surface, which can evaporate some materials on the surface. Therefore, higher energy density causes more evaporation and, hence, more tensile stress on the surface. However, a high enough irradiation energy density tends to etch the surface of the alumina plates.

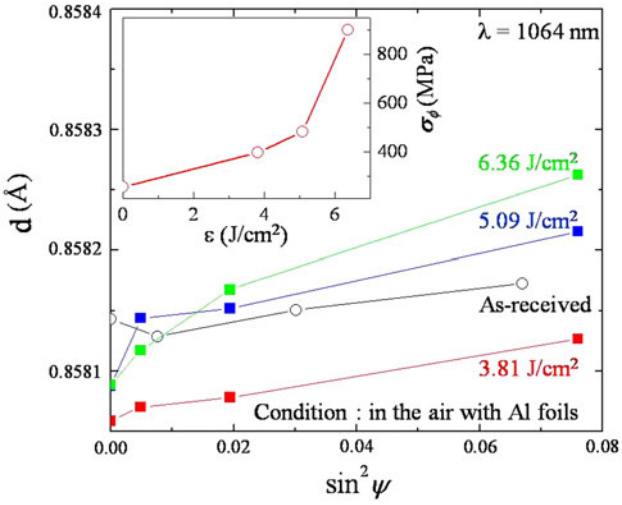

Fig. 3 The interplanar spacing versus $\sin^2\psi$ by change of energy density λ = 1064 nm. The *inset* summarizes the relation between residual stress and energy density

Since photon energy at λ = 532 nm is considerably higher than that at λ = 1064 nm, the irradiation conditions should be adjusted to prevent damaging the alumina plates. In order to investigate the effect of irradiation conditions on the residual stress of the alumina plates, the samples were irradiated under various conditions, for example, by changing the energy density, irradiating in a water jacket, enveloping the samples with Al foils, and so forth. Among those conditions, the samples irradiated with an energy density of 12.7 J/cm^2 in a water jacket without Al foils exhibit the largest tensile residual stress. Figure 4 shows $d_\psi(\sin^2\psi)$ for different scan times at the same energy density, 12.7 J/cm^2. Though it is expected that increasing the scan time increases the slope of $d_\psi(\sin^2\psi)$, there is no systematic change in the slope with increasing scan time. The reason will be discussed in the next section. The residual stresses are estimated again by the $\sin^2\psi$ technique. The evaluated residual stresses by a one time scan, a two times scan, and a four times scan are ~848, ~75, and ~300 MPa, respectively. This indicates that the residual stress can be controlled, and the residual stress is sensitive to the irradiation conditions. Figure 5 shows $d_\psi(\sin^2\psi)$ for the other irradiation conditions. The solid circles and diamonds correspond to data obtained by enveloping the samples by Al foils and irradiating them in water, respectively. The residual stress estimated by a one time scan is higher (~421 MPa) than that (~69 MPa) by a two times scan. This result is consistent with that obtained by irradiating the samples without Al foils, as shown in Fig. 4. When an alumina plate is irradiated in air without an Al foil with an energy density of 3 J/cm^2, the residual stress is about 590 MPa. Note that, in the case of λ = 532 nm, when the alumina plates are irradiated in air without the Al foils with an energy density over 3 J/cm^2, the surfaces of the plates get etched.

3.2 Surface Morphology

An SEM is one of the most powerful tools to investigate the surfaces of alumina plates irradiated by laser beams. All the alumina grains of the as-received alumina plate have sharp edges because the manufacturing process such as grinding breaks or splits alumina grains, as shown in Fig. 6(a). However,

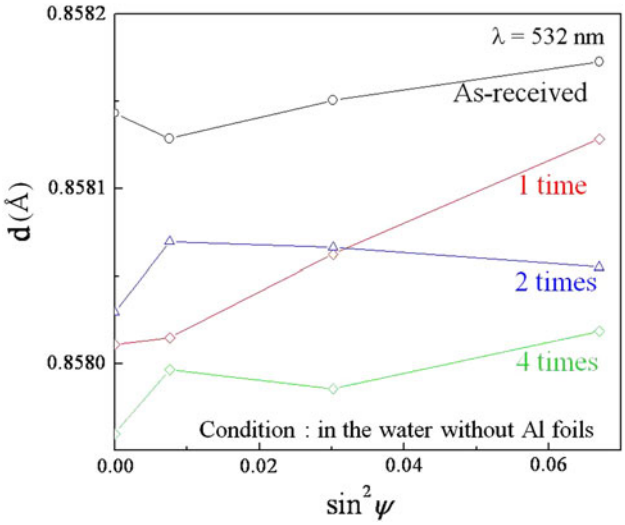

Fig. 4 Residual stress change by the scan time for λ = 532 nm

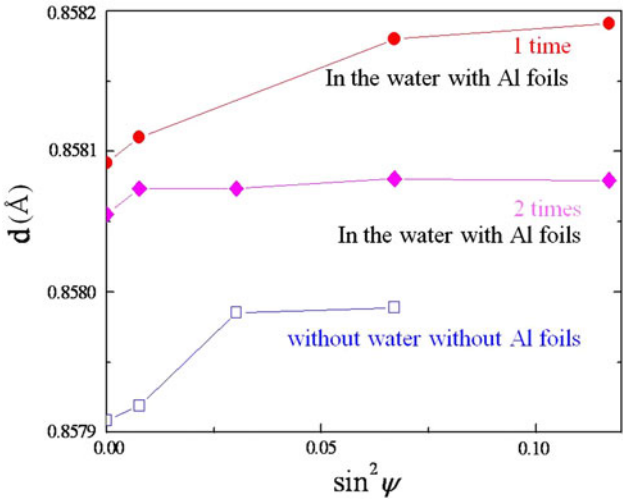

Fig. 5 $d_{\psi}(\sin^2\psi)$ for other irradiation conditions of λ = 532 nm

when the laser beam of λ = 1064 nm irradiates the alumina plates enveloped by the Al foils, the sharp edges of the alumina grains get deformed according to the irradiation energy density. Figure 6(b), (c), and (d) shows the SEM images at the irradiation energy densities of 3.81, 5.09, and 6.36 J/cm^2, respectively. Since Al foils have a good thermal conductivity, the thermal energy of laser beam directly affects the contact areas, which are the likely edges of the grains. Thus, when the energy density is increased, the sharp edges of the grains get further deformed, as shown in Fig. 6(b)-(d). Though the energy density is 6.36 J/cm^2, the sharp edges of the grains can be observed in the inner region where the Al foil is not attached, as shown in Fig. 6(d). Since alumina is a good thermal insulator, the inside grains can be preserved during the laser irradiation.

Figure 7(a)-(c) shows SEM images of samples irradiated with λ = 532 nm at an energy density of ~12.7 J/cm^2 in water without Al foils. The SEM image obtained by a one time scan (Fig. 7a) shows that the edges of alumina plates are destroyed by the irradiation. The second laser irradiation of the alumina plates results in the formation of many pores on the grains,

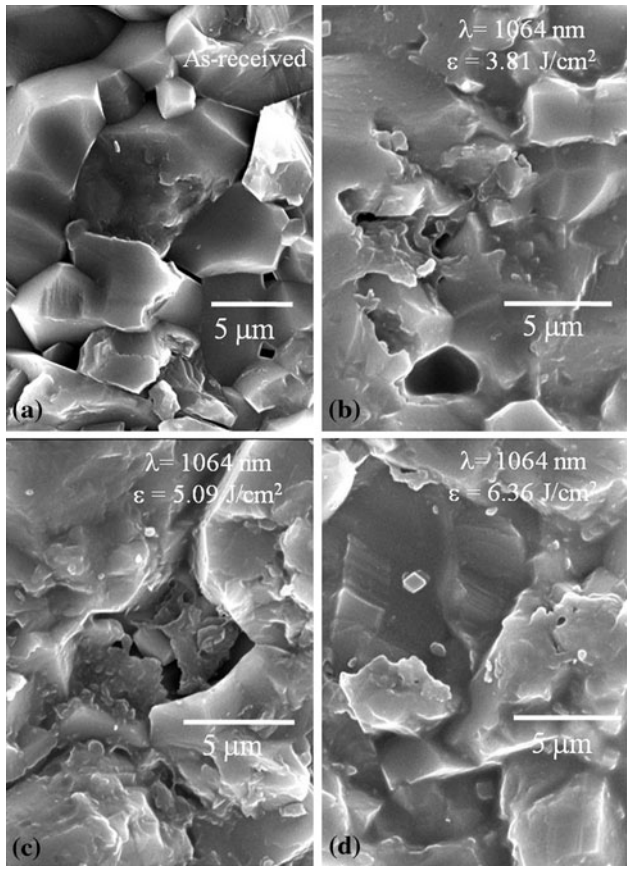

Fig. 6 The change in surface morphology after irradiation by a laser beam with λ = 1064 nm. (a) The SEM image of the as-received sample. The SEM image of alumina plates irradiated by the energy densities (b) ε = 3.81 J/cm^2, (c) ε = 5.09 J/cm^2, and (d) ε = 6.36 J/cm^2

shown in Fig. 7(b). The presence of pores indicates that the some parts of alumina surfaces have melted by the second laser irradiation. Further, the difference in the densities of solid and liquid alumina causes partial cracking of the surface due to mechanical tension. This is called laser-induced explosive boiling, which often occurs under high-power nanosecond laser irradiation (Ref 20, 21). Results of the four times scan show that an increase in the scan time increases the number of pores on the surface (Fig. 7c). As discussed earlier, the residual stress of the two and four times scanned samples is considerably less than that of the one time scanned sample. Since the pores are formed by the cracking of the alumina surface because of the density difference between solid and liquid alumina, the high tensile residual stress induced by the first laser irradiation should be relieved. When laser irradiation is performed without water and Al foils, the edges of the grains are severely deformed, and the tiny alumina debris can be observed on all the surfaces, as shown in Fig. 7(d). Figure 8(a) and (b) shows SEM images of the samples enveloped by Al foils and irradiated by a laser beam with λ = 532 nm in water. As compared to the one time scan, as shown in Fig. 8(a), the two times scan causes severe deformation of the edges of the grains. However, in this case, the edges of the inside grains are not affected by the laser irradiation. Again, this can be attributed to the good thermal conduction of Al foils and the good thermal insulation of alumina.

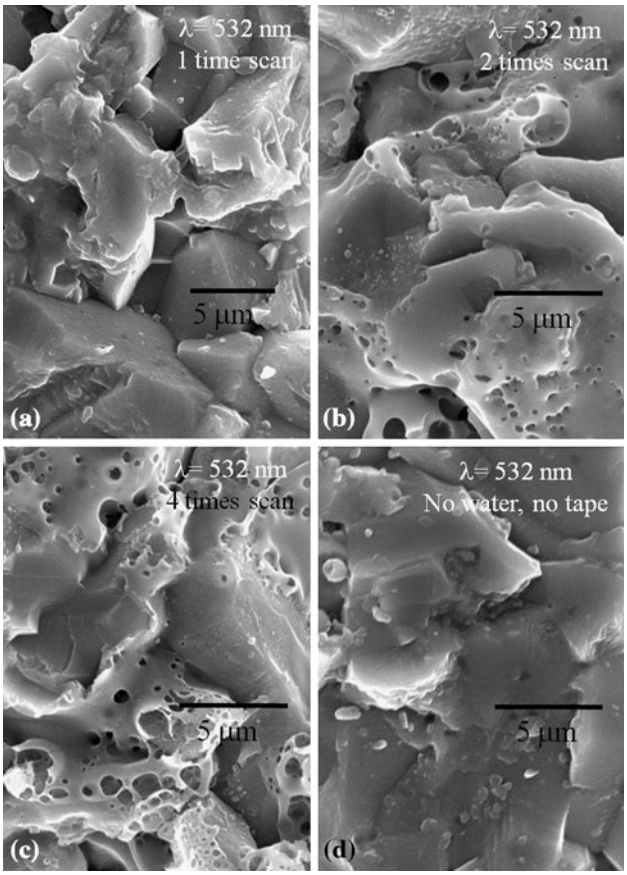

Fig. 7 The change in surface morphology after irradiation by a laser beam with λ = 532 nm. The SEM image of a (a) one time scan, (b) two times scan, and (c) four times scan. (d) The SEM image of alumina plates irradiated in air without aluminum foils

In the case of the samples irradiated by λ = 532 nm in water, increasing the scan time increases the number of pores on the surface, indicating an increase in the surface roughness, which surface roughness measurements have proved. The average surface roughness of the as-received sample is 1.11 μm. The average surface roughnesses obtained by the one time scan, two times scan, and four times scan are 1.37, 1.7, and 3.07 μm, respectively. In the case of the samples irradiated by λ = 1064 nm, the average surface roughness for the energy densities of 3.81, 5.09, and 6.36 J/cm^2 are 1.82, 1.13, and 1.11 μm, respectively. This result can be expected from the SEM images, because the increased energy density deforms the sharp edges of the grains severely, indicating that the surface roughness decreases with the increasing energy density. All the SEM images and the surface roughness data suggest that the surface status strongly depends on the laser irradiation conditions.

Laser irradiation gives rise to tensile residual stress. In general, tensile residual stress is increased by the heating and cooling of surfaces. In the case of the fundamental wave of a Q-switched Nd:YAG laser, the wavelength (λ = 1064 nm) belongs to the infrared range and, hence, the irradiation causes the heating of the samples. Further, Al foils can dissipate the heat from the samples causing tensile residual stress. It is noted that the two times scan using λ = 532 nm greatly reduced tensile residual stress, indicating that the residual stress can be

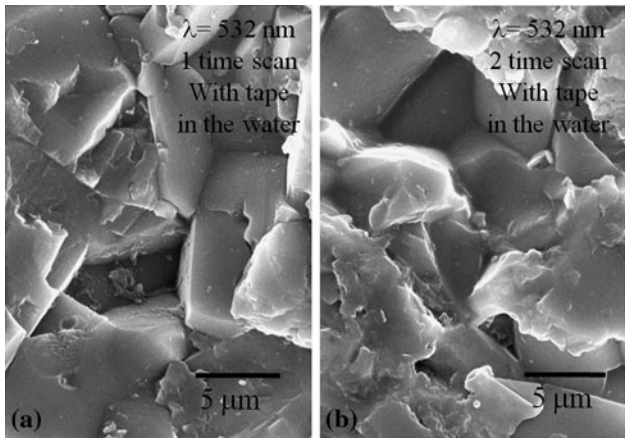

Fig. 8 The SEM image of Al_2O_3 irradiated by λ = 532 nm with aluminum foils in water. The SEM image of a (a) one time scan and (b) two times scan

controlled by modifying the irradiation conditions. Sometimes, certain applications require a high tensile residual stress. For example, to improve the mechanical properties of Al_2O_3, a glass infiltration method (Ref 20, 22) with silicate glass is used. However, the compressive stress of the layers fabricated by this method is so high that the surface sometimes gets delaminated. In such a case, it is necessary to relieve compressive residual stress by applying laser treatments.

4. Conclusions

Residual stress and surface morphology changes in alumina plates irradiated by 1064 and 532 nm laser pulses from a Nd:YAG laser were investigated. Residual stress and surface morphology are sensitive to the irradiation conditions such as wavelength, energy density, scan time, and the presence of Al foils or water. Laser irradiation of the alumina plates induces tensile residual stress, which increases in proportion to increasing energy density. Increasing the scan time by maintaining the energy density constant at the value that yields the largest tensile stress does not increase residual stress. The SEM images and average surface roughness of the samples are seriously affected by the laser irradiation conditions.

Acknowledgments

This research was supported by Development of Key Technologies for Nuclear Hydrogen, Proton Engineering Frontier Project sponsored by the Ministry of Education, Science and Technology (MEST), and by a grant from the Fundamental R&D program from Core Technology of Materials funded by the Ministry of Knowledge Economy (MKE), Republic of Korea.

References

1. D. Triantafyllidis, L. Li, and F.H. Stott, The Effects of Laser-Induced Modification of Surface Roughness of Al_2O_3-Based Ceramics on Fluid Contact Angle, *Mater. Sci. Eng. A*, 2005, **390**, p 271–277
2. J. Lawrence, Identification of the Principal Elements Governing the Wettability Characteristics of Ordinary Portland Cement Following

High Power Diode Laser Surface Treatment, *Mater. Sci. Eng. A*, 2003, **356**, p 162–172
3. J. Lawrence and J. Li, *Laser Modification of Wettability Characteristics of Engineering Materials*, 1st ed., Professional Engineering Publishing, London, 2001
4. A.H. Heuer, Oxygen and Aluminum Diffusion in α-Al_2O_3: How Much Do We Really Understand? *J. Eur. Ceram. Soc.*, 2008, **28**, p 1495–1507
5. B. Dhupal, B. Doloi, and B. Bhattacharyya, Pulsed Nd:YAG Laser Turning of Micro-Groove on Aluminum Oxide Ceramic (Al_2O_3), *Mach. Tools Manufact.*, 2008, **48**, p 236–248
6. D. Triantafyllidis, J.R. Bernstein, L. Li, and F.H. Stott, Dual Laser Beam Modification of High Alumina Ceramics, *J. Laser Appl.*, 2002, **15**, p 49–54
7. A.G. Evans and J.W. Hutchinson, The Thermomechanical Integrity of Thin Films and Multilayers, *Acta Metall. Mater.*, 1995, **43**, p 2507–2530
8. J.W. Hutchinson and Z. Suo, Mixed Mode Cracking in Layered Materials, *Adv. Appl. Mech.*, 1992, **29**, p 63–191
9. I.C. Noyan and J.B. Cohen, *Residual Stress Measurement by Diffraction and Interpretation*, Springer, New York Inc, 1987
10. X.J. Zheng, J.J. Li, and Y.C. Zhou, X-ray Diffraction Measurement of Residual Stress in PZT Thin Films Prepared By Pulsed Laser Deposition, *Acta Mater.*, 2004, **52**, p 3313–3322
11. X.J. Zheng, Y.C. Zhou, and J.J. Li, Nano-Indentation Fracture Test of $Pb(Zr_{0.52}Ti_{0.48})O_3$ Ferroelectric Thin Films, *Acta Mater.*, 2003, **51**, p 3985–3997
12. R. Arvind Singh, A.K. Sood, V. Jayaram, and S.K. Biswas, Analysis of Microresidual Stresses in 6H-SiC Particles Within Al_2O_3-SiC-(Al, Si) CMC Using Raman Spectroscopy, *Scripta Mater.*, 1997, **38**, p 617–622
13. W. Xu, D. Lu, and T. Zhang, Determination of Residual Stresses in Pb(Zr0.53Ti0.47)O3 Thin Films With Raman Spectroscopy, *Appl. Phys. Lett.*, 2001, **79**, p 4112–4114
14. D.B. Hovis and A.H. Heuer, Confocal Photo-Stimulated Microspectroscopy (CPSM)-Residual Stress Measurements in Al_2O_3 Using Confocal Microscopy, *Scripta Mater.*, 2005, **53**, p 347–349
15. A.N. Samant and N.B. Dahotre, Multilevel Residual Stress Evaluation in Laser Surface Modified Alumina Ceramic, *Appl. Phys. A*, 2008, **90**, p 493–499
16. W.A. Rachinger, A Correction for the α_1, α_2 Doublet in the Measurement of Widths of x-ray Diffraction Lines, *J. Sci. Instrum.*, 1948, **25**, p 254–255
17. D.P. Koistinen and R.E. Marburger, A Simplified Procedure for Calculating Peak Position in x-ray Residual Stress Measurements on Hardened Steel, *Trans. ASM*, 1959, **51**, p 537
18. C. Meade and R. Jeanloz, Yield Strength Al_2O_3 of at High Pressures, *Phys. B*, 1990, **42**, p 2532–2535
19. V.R. Vedula, S.J. Glass, D.M. Saylor, G.S. Rohrer, W.C. Carter, S.A. Langer, and E.R. Fuller, Residual-Stress Predictions in Polycrystalline Alumina, *J. Am. Ceram. Soc.*, 2001, **84**, p 2947–2954
20. J.S. Xiang, X. Hui, H.J. Zhi, and L.W. Yong, Preparation of Glass-Infiltrated 3Y-TZP/Al_2O_3/Glass Composites, *Mater. Lett.*, 2004, **58**, p 1750–1753
21. Q. Lu, S.S. Mao, X. Mao, and R.E. Russo, Delayed Phase Explosion During High-Power Nanosecond Laser Ablation of Silicon, *Appl. Phys. Lett.*, 2002, **80**, p 3072–3074
22. M. Guazzato, M. Albakry, Q. Linda, and M.V. Swain, Influence of Surface and Heat Treatments on the Flexural Strength of a Glass-Infiltrated Alumina/Zirconia-Reinforced Dental Ceramic, *Dent. Mater.*, 2005, **21**, p 454–463